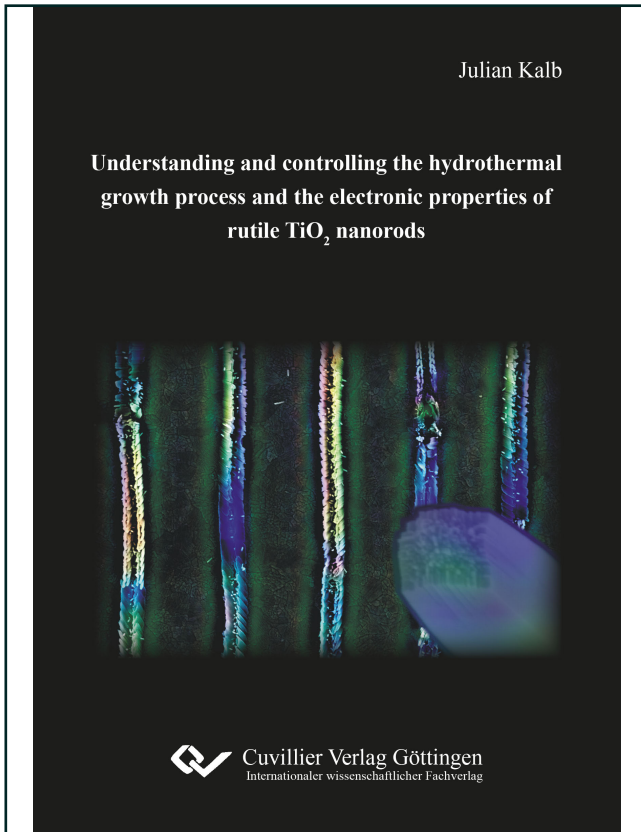




Julian Kalb (Autor)

Understanding and controlling the hydrothermal growth process and the electronic properties of rutile TiO₂ nanorods



<https://cuvillier.de/de/shop/publications/8149>

Copyright:

Cuvillier Verlag, Inhaberin Annette Jentzsch-Cuvillier, Nonnenstieg 8, 37075 Göttingen, Germany

Telefon: +49 (0)551 54724-0, E-Mail: info@cuvillier.de, Website: <https://cuvillier.de>



Contents

Abstract	1
1 Introduction	5
2 Basics of Titanium Dioxide	11
2.1 Exploitation and Economic Meaning of TiO ₂	11
2.2 Crystal Properties of Rutile and Anatase TiO ₂	15
2.2.1 Morphologies and Crystal Structure	15
2.2.2 Crystal Defects	16
2.2.3 Surface Science of TiO ₂	17
2.2.4 Crystal Dynamics and Thermal Properties	18
2.3 Phase Transitions in TiO ₂ /Substrate Systems	23
2.3.1 Anatase-to-Rutile Phase Transition in Bulk TiO ₂	23
2.3.2 Anatase-to-Rutile Phase Transition in Nanocrystalline TiO ₂	28
2.4 Extended Definition of Optical, Electronic, and Optoelectronic Properties of TiO ₂ Semiconductors	37
2.4.1 Optical Properties	38
2.4.2 Electronic Properties	38
2.4.3 Optoelectronic Properties	39
2.5 Optical Properties of TiO ₂	40
2.5.1 Refractive Index and Dielectric Function	40
2.5.2 Light Scattering on Spherical TiO ₂ Nanoparticles	42
2.5.3 Dielectric Light Scattering on Highly Anisotropic Nanoparticles	43
2.5.4 An Ordered Array of Nanoparticles as a Basic Module of Metamaterials	45
2.5.5 Disordered Assemblies of Nanoparticles as an Effective Medium	46
2.6 Electronic Properties of Bulk and Nanostructured TiO ₂	47
2.6.1 Band Structure in Bulk TiO ₂	47
2.6.2 Chemical Potential and Electron Density in Intrinsic Semiconductors	48
2.6.3 Chemical Potential and Electron Density in n-type TiO ₂	49
2.6.4 Band-Derived Effective Mass of Electrons	50
2.6.5 Conductivity and Mobility of Electrons in TiO ₂	50
2.6.6 Electronic States and Conductivity in Doped TiO ₂	60
2.6.7 Electronic States and Conductivity on Surfaces and Grain Boundaries in TiO ₂	68
2.6.8 Electronic States and Conductivity in TiO ₂ Nanoparticles	71
2.7 Static Transient Current Effects in TiO ₂	75
2.7.1 Band Bending at the Metal-Semiconductor Interface	75
2.7.2 Electrode-Limited Conduction Mechanisms	81
2.7.3 Bulk-Limited Conduction Mechanisms	84
2.7.4 Effects of Structure Size on the Transient Current	91
2.7.5 Effects of the Fabrication Technique on the Transient Current	92
2.7.6 Effects of Post-Treatment on the Transient Current in TiO ₂	92



2.8	Time-Dependent Transient Current Effects in TiO ₂	95
2.8.1	Capacitive Effects	96
2.8.2	Inelastic Electron-Phonon Scattering and Joule Heating	97
2.8.3	Trapping and Detrapping of Electrons	98
2.8.4	Drift Velocity Effects	101
2.8.5	Oxide Degradation	101
2.8.6	Localized Resistive Switching Behavior	106
2.8.7	Effect of Adsorbates	107
2.9	Optoelectronic Properties of TiO ₂	109
2.9.1	Excitation of Optical Phonons	109
2.9.2	Excitation of Bound Charge Carriers	109
2.9.3	Electron Injection via Adsorbates	112
2.9.4	Light-Controlled Density of Mobile Electrons	112
2.9.5	Excitation of Mobile Electrons	113
2.9.6	Photoconductivity and Photocurrent	113
2.9.7	Internal Photoemission	113
3	Manufacturing of TiO₂ Nanostructures	115
3.1	Thin TiO ₂ Films	115
3.1.1	Sputter Deposition	115
3.1.2	Laser Ablation	115
3.1.3	Electron-Beam Evaporation	116
3.1.4	Spray Pyrolysis	116
3.1.5	Sol-gel Method	117
3.1.6	Atomic Layer Deposition	117
3.1.7	TiCl ₄ Treatment	117
3.2	Hydrothermal Growth of Rutile TiO ₂ Nanorods	118
3.2.1	The Conversion of the Precursor into TiO ₂	118
3.2.2	The Rutile TiO ₂ Crystal Shape at Thermodynamic Equilibrium Condition	120
3.2.3	Formation of Branches	120
3.2.4	Substructure of Full-grown TiO ₂ Nanorods	121
3.2.5	Substrates for the Hydrothermal Growth of Rutile TiO ₂ Nanorods	123
3.2.6	Toxicity of the Investigated TiO ₂ Nanostructures	123
4	Experimental Methods	125
4.1	Fabrication Techniques	125
4.1.1	Substrates	125
4.1.2	Rutile and Anatase TiO ₂ Films/ Seed Layers	125
4.1.3	Hydrothermal Growth of Rutile TiO ₂ Nanorods	129
4.1.4	Lithography	129
4.1.5	Fabrication of Polystyrene Sphere Monolayers (PSML)	131
4.1.6	Focused Ion Beam (FIB) Milling	132
4.1.7	Scanning Probe Lithography	132
4.1.8	Laser Lithography	132
4.2	Characterization Techniques	133
4.2.1	Standard Characterization Techniques	133
4.2.2	Electronic Properties	135
4.2.3	Optical Properties	136



5	Thin TiO₂ Films and Seed Layer for the Hydrothermal Method	139
5.1	Thin Anatase TiO ₂ Seed Layers	140
5.1.1	Anatase Polycrystalline TiO ₂ Films Made by Sputter Deposition	140
5.1.2	Anatase Polycrystalline TiO ₂ Films Made by Spray Pyrolysis	144
5.1.3	Anatase Polycrystalline TiO ₂ Films Made by SALD	144
5.2	Thin Rutile TiO ₂ Seed Layers	145
5.2.1	Polycrystalline Rutile TiO ₂ Films Made by Sputter Deposition	145
5.2.2	Polycrystalline Rutile TiO ₂ Films Made by Electron-Beam Evaporation	146
5.2.3	Polycrystalline Rutile TiO ₂ Films Made by a Sol-gel Method	148
6	Hydrothermal Growth of Rutile TiO₂ Nanorods on Rutile and Anatase Films	149
6.1	Hydrothermal Growth in Solution	150
6.2	Hydrothermal Growth on Rutile Seed Layers	153
6.2.1	Hydrothermal Growth on Macroscopic Rutile TiO ₂ Single Crystals	153
6.2.2	Hydrothermal Growth on Sputtered, Sol-gel, and Evaporated Rutile TiO ₂ Seed Layers	157
6.2.3	Hydrothermal Growth on Rutile FTO Seed Layers	159
6.3	Hydrothermal Growth on Anatase Seed Layers	160
6.3.1	Hydrothermal Growth on Sputtered Fine-Grained Anatase TiO ₂ Seed Layers	160
6.3.2	Hydrothermal Growth on Coarse Grain Sputtered and Sprayed Anatase TiO ₂ Seed Layers	161
6.4	Stages of the Hydrothermal Growth Process	164
6.4.1	Nucleation	164
6.4.2	Period of Crystal Growth	165
6.4.3	Ostwald Ripening	166
6.4.4	One- and Multi-directional Growth (Branching)	167
7	Non-Equilibrium Growth Model for Fibrous Rutile TiO₂ Nanorods	171
7.1	Model for the Origin of the Typical Fine Structure in Rutile TiO ₂ Nanorods	172
7.1.1	Facet-Dependent Crystallization Speeds	172
7.1.2	Facet-Dependent Growth Speeds Corresponding to Wulff Construction	172
7.1.3	Non-Equilibrium Growth Model Describing the Origin of the Fine Structure	172
7.1.4	From Polycrystalline Fine Structure Towards Single Crystal	174
7.2	Observable Consequences of the Non-Equilibrium Growth Model	175
7.2.1	Attachment of Fingers	175
7.2.2	Dependence of the Finger's Diameter on the Process Temperature	177
7.2.3	Post-Growth Atomic Rearrangement in Hydrochloric Acid	178
7.2.4	Post-Growth Annealing in Different Atmospheres	179
8	Expanding the Horizon of Position-Controlled Hydrothermal Growth Methods	183
8.1	From Standard Methods to New Advanced Lithography Techniques	184
8.2	Confined TiO ₂ NRAs Made by Optical Contact Lithography	184
8.2.1	Standard Structures	184
8.2.2	Levitating TiO ₂ NRAs	184
8.3	Double Superlattice by Optical Lithography and PSML	185
8.4	Confined TiO ₂ NRAs Made by Electron-Beam Lithography	188
8.5	Focused Ion Beam Triggered Growth of TiO ₂ Nanorods	189
8.5.1	Focussed Ion Beam Milling	189
8.5.2	Confined NRAs Made by Focused Ion Beam Milling	190



8.6	Advanced Scanning Probe Lithography Using Anatase-to-Rutile Transition of Localized Nanoparticles	193
8.6.1	Advanced Scanning Probe Lithography	194
8.6.2	Excluding Competing Processes Resulting in Localized Growth of Nanorods	194
8.6.3	Special Features of the Presented Advanced Scanning Probe Lithography	196
9	LASER-Induced Position-Controlled Hydrothermal Growth	199
9.1	Basics about Laser Lithography Techniques	199
9.1.1	Formation of Interlayer between TiO ₂ and Silicon Substrates	199
9.1.2	Light In-Coupling in Anatase and Rutile TiO ₂ Films	201
9.1.3	Absorption of Incident Light	208
9.1.4	Heat Dissipation in the Silicon/TiO ₂ Interface Region	209
9.1.5	Melting Parameters	210
9.1.6	Recrystallization Process	211
9.2	Results and Discussion of Laser Lithography Techniques	213
9.2.1	Laser-Induced Oxidation Lithography	213
9.2.2	cw Laser-Induced Melting Lithography (CiMeL)	215
9.2.3	High Energy cw Laser-Induced Melting Lithography (HELM)	215
9.2.4	Low Energy cw Laser-Induced Melting Lithography (LELM)	217
9.2.5	Pulsed Laser-Induced Pattern Generation	219
10	Optical Properties of Rutile TiO₂ Nanostructures	237
10.1	Scattering of Individual TiO ₂ Nanorods	240
10.1.1	Polarization-Dependent Scattering on Individual Nanorods	241
10.1.2	Size Effects on Light Scattering	242
10.1.3	Increasing Light Scattering with the Orientation of Nanorods	244
10.2	Scattering Superlattices Fabricated with Optical Contact Lithography	244
10.2.1	Scattering at Levitating NRA Membranes	244
10.3	Scattering on Narrow Linear NRA	247
10.3.1	Scattering at Superlattices Fabricated with Electron-Beam Lithography	247
10.3.2	Scattering Superlattices Fabricated by Scanning Probe Lithography	250
10.3.3	Scattering at Laser-Fabricated Superlattices	252
11	Time Evolution of the Transient Current in TiO_{2-x} Nanocrystals	255
11.1	General Model for the Electron Transport in As-Grown Rutile TiO _{2-x} Nanorods	257
11.1.1	Separating the Rod into an Upper and a Bottom Part	257
11.1.2	The Effect of CVS on the Electronic Landscape	258
11.1.3	A Simplified Model for $I - V$ Measurements	261
11.2	General Model for the Electron Transport in Annealed Rutile TiO _{2-x} Nanorods	263
11.2.1	The Effect of Annealing in Vacuum on the Electronic Landscape	263
11.2.2	The Effect of Annealing in Oxygen on the Electronic Landscape	263
11.3	Electron Transport in Specific Structures	265
11.3.1	Rutile TiO _{2-x} Nanorods Grown at 150 °C (NR150)	265
11.3.2	Rutile TiO _{2-x} Nanorods Grown at 180 °C (NR180)	273
11.3.3	Rutile TiO _{2-x} Nanorods Grown at 220 °C (NR220)	277
11.3.4	Rutile TiO _{2-x} Nanorods Grown at 180 °C and treated with hot hydrochloric acid (HCL180)	279
11.3.5	Rutile TiO _{2-x} Nanotubes Grown at 180 °C and etched with hot hydrochloric acid (NT180)	281
11.3.6	TiO _{2-x} Films Deposited via Sputter Deposition (FI)	284



11.3.7 The Effect of Adsorbed Oxygen on The Transient Current	286
12 Conclusion and Outlook	289
13 Appendix	297
13.1 Chapter 5	297
13.1.1 Thin Seed Layers Made of Different Rutile Materials	297
13.2 Chapter 6	299
13.2.1 Hydrothermal Growth on TiCl_4 Treatment Processed Seed Layers	299
13.2.2 Hydrothermal Growth on Reduced WO_3 Seed Layers	299
13.2.3 Hydrothermal Growth on ALD and SALD Seed Layers	300
13.2.4 Probing the Rutile Phase with Hydrothermal Growth	301
13.2.5 Crystal Structure and Hydrothermal Growth on Rutile/Anatase Sand- wiches	301
13.3 Chapter 8	303
13.3.1 Double Superlattice by Optical Lithography and PSML	303
13.3.2 Applying Scratching on Reduced WO_3 Films	303
13.4 Chapter 9	305
13.4.1 Correlation Between Provided Beam Energy and Melting Behavior for cw Laser Melting	305
13.4.2 Suppressing Hydrothermal Growth by Intensive Electron-Beam Exposure	305
13.5 Chapter 10	307
13.5.1 Scattering on Superstructures Made by PSML	307
13.5.2 Intensity Pattern Occurring Near the Nanowalls	307
13.6 Chapter 11	310
13.6.1 Experimental Characteristics	310
13.6.2 The Influence of Further Effects on the Time-Dependent Charge Transport Behavior	317
Glossary	319
List of Symbols	325
List of Acronyms	327
List of Figures	329
List of Tables	333
References	335
Subject Index	411
List of scientific Output and Projects	421
Acknowledgment	427